The ROYAL COLLEGE of
OPHTHALMOLOGISTS

Check for updates

ARTICLE

Predictive role of optical coherence tomography angiography for exudation recurrence in patients with type 1 neovascular age-related macular degeneration treated with pro-re-nata protocol

Mihyun Choi[1], Seong-Woo Kim [ID][1][✉], Cheolmin Yun[2], Jong-Hyun Oh[3] and Jaeryung Oh[4]

OBJECTIVES: We sought to identify the consecutive changes and predictive features for exudation recurrence in macular neovascularization (MNV) using optical coherence tomography angiography (OCTA) in type 1 neovascular age-related macular degeneration (NVAMD).
METHODS: A total of 291 OCTA images in consecutive visit of 45 patients newly diagnosed with type 1 NMV and treated with three loading intravitreal anti–vascular endothelial growth factor injections (IVIs) and a pro-re-nata (PRN) therapy regimen were analysed. Quantitative features of OCTA included the MNV area, MNV length, total number of endpoints (open-ended vessels) and junctions (internal branching) using AngioTool. Two subgroups were divided according to exudation recurrence time from the third IVI (group 1: ≤3 months vs. group 2: >3 months).
RESULTS: The area, length, number of total junctions, and endpoints decreased during three loading IVIs and increased at exudation recurrence (all $p < 0.05$). In a subgroup analysis of consecutive OCTA images, the number of total endpoints increased at two months prior to exudate recurrence in group 2 (the late recurrence group, $p = 0.020$). A higher total number of endpoints of MNV at baseline were found to be related with group 1 (early recurrence, $p = 0.020$ and 0.012 in univariate and multivariate regression analyses).
CONCLUSIONS: The MNV with higher open-ended vessels at the lesion periphery at baseline might be expected to show earlier recurrence of exudation after loading IVIs. By observing the number of open-ended vessels in consecutive OCTA images, exudation recurrence could be predicted.

Eye (2023) 37:34–41; https://doi.org/10.1038/s41433-021-01879-2

INTRODUCTION

Anti-vascular endothelial growth factor (anti-VEGF) treatments have improved the prognosis of patients with neovascular (NV) age-related macular degeneration (NVAMD), a leading cause of blindness among elderly patients [1]. Although the efficacy of anti-VEGF treatments such as ranibizumab and aflibercept has been demonstrated through randomized clinical trials based on regular, fixed-dose protocols [2, 3], various treatment regimens have been used clinically, including pro-re-nata (PRN), treat and extend (T&E), and treat–extend–stop, to reduce treatment burden [4, 5].

However, a recent real-world prospective study by LUMINOUS that included a large patient population from 42 countries reported that there were variable diagnosis to treatment times (1–49 days) and a variable number of injections performed in one year (2.7–8.7 injections) due to the diversity of medical environments in each country [6]. Considering the real-world clinics, there is a need to predict frequent recurrence in such patients to

facilitate the determination of appropriate treatment intervals and to identify preceding changes in multimodal images prior to exudation recurrence.

Recent advances in optical coherence tomography angiography (OCTA), a novel and noninvasive imaging technique for macular neovascularization (MNV), have suggested the possibility of using OCTA to guide treatment [7–9]. In previous studies, MNV with exudation was reported to decrease in terms of the area, segment length, and fractal dimensions after anti-VEGF treatment, while these same metrics were increased when exudation recurred [10–12]. However, little is known about the characteristics of MNV that predict frequent exudation recurrence and few reports on the time-course of changes in MNV in consecutive patients exist.

The primary purpose of this study was to investigate whether there are quantitative characteristics in treatment-naïve type 1 MNV related to early exudation recurrence after three loading IVIs. Further, we assessed quantitative changes in type 1 MNV in

[1]Department of Ophthalmology, Korea University Guro Hospital, 148, Gurodong-ro, Guro-gu, Seoul 08308, Republic of Korea. [2]Department of Ophthalmology, Korea University Ansan Hospital, 123, Jeokgeum-ro, Danwon-gu, Ansan-si, Gyeonggi-do, Republic of Korea. [3]Department of Ophthalmology, Dongguk University, Ilsan Hospital, 27, Dongguk-ro, Ilsandong-gu, Goyang-si, Gyeonggi-do, Republic of Korea. [4]Department of Ophthalmology, Korea University Anam Hospital, 145, Anam-ro, Seongbuk-gu, Seoul, Republic of Korea. ✉email: ksw64723@korea.ac.kr

treatment-naïve NVAMD patients during IVIs and the recurrence of exudation to discern in which order the sequential relationship of changes among features occurred. By doing so, the OCTA changes in MNV that preceded exudation on structural OCT images can be specified and, thus, identified earlier on.

MATERIALS AND METHODS
This retrospective cohort study reviewed medical records and 291 OCTA images from consecutive visit of 45 patients with NVAMD who visited the Korea University Guro Hospital between February 2018 and July 2021. The institutional review board of Korea University Medical Centre approved this study and all research processes were conducted in accordance with the tenets of the Declaration of Helsinki. The institutional review board of Korea University Medical Centre waived the need to collect written informed consent from the participants because of the study's retrospective design.

Patient selection
Among patients older than 50 years who were diagnosed with subfoveal type 1 NVAMD by multimodal imaging (fluorescein angiography [FA], indocyanine green angiography [ICGA], and structural OCT), treated with intravitreal aflibercept (Eylea; Regeneron Pharmaceuticals, Tarrytown, NY, USA) injections, and who exhibited complete drying on structural OCT images after three loading injections were included. Patients who were followed for one year after their third IVI were included. Patients with type 2 or 3 NV or polypoidal choroidal vasculopathy, large pigment epithelial detachment (PED) resulting in severe OCTA segmentation error, any concurrent vascular obstructive retinal disease, or a history of any treatment for NVAMD were excluded. Patients with history of central serous chorioretinopathy, trauma, medication usage related with retinal pigment epithelium (RPE) disruption, or moderate to high myopia (> −3.00 dioptres of spherical equivalent) also were excluded.

Visit and OCTA image examination
The patient treatment and visit protocols adopted in our practice are presented in eFig. 1. All patients received three monthly loading IVIs and visited the clinic within one month after each injection. We defined the OCTA of the visits as T1, T2, and T3, respectively. At baseline (treatment naïve) and T3, FA and ICGA were performed and the area of type 1 MNV as a plaque-like staining lesion on venous intermediate phase ICGA (5-7 minutes) [13] was manually measured (eFig. 2) using the software (HEYEX; Heidelberg Engineering, Heidelberg, Germany). When dry-up on structural OCT images was confirmed at T3 (one month after the third IVI was performed), patients were followed for every two months (± 1 week) and an additional IVI was performed if exudation in structural OCT presented according to the PRN protocol [5]. Best corrected visual acuity (BCVA), slit-lamp examination, and dilated funduscopic examination were performed, and spectral-domain OCT and OCTA images were obtained at each visit.

OCTA imaging at the recurrence of exudation after the third loading injection was defined as R (recurrence) and that at one month after the fourth IVI was defined as T4. Among the patients who received treatment according to this visit protocol, only one eye from each patient and those who followed the visit protocol until T4 were included in the analysis. Subgroup analysis was conducted by stratifying the patients wherein the timing of exudation recurrence on structural OCT images within two months from T3 as group 1 (right after T3, early recurrence) and that where it was within more than two months as group 2 (late recurrence). We defined the OCTA image two month before exudation recurrence as P (preceding exudation) among patients in group 2. Data including the Logarithm of the Minimum Angle of Resolution (logMAR) BCVA and additional number of IVIs received in one year after the three loading injections were evaluated in patients who were followed up with for a longer period.

OCTA image acquisition
OCTA images were obtained using the Spectralis OCT2 spectral-domain OCT device (Heidelberg Engineering, Heidelberg, Germany), which can acquire 4.3 × 4.3 mm (15° × 15°) angiography scans, with a wavelength of 870 nm, lateral resolution of 11.4 μm/pixels, and axial resolution of 3.87 μm/pixels. OCTA images with artifacts such as shadows, double vessel patterns, or horizontal movement lines were excluded from the study analysis [14]. Automatic segmentation was performed using the software

(HEYEX; Heidelberg Engineering, Heidelberg, Germany) and the en-face (C-scan) images of MNV were defined from the external limiting membrane to the line of Bruch's membrane [15]. In fusion images of structural OCT and the corresponding blood flow signal (structural OCT + OCTA), visual correlation of structural and flow signal was established. Manual segmentation defining upper and lower boundaries of the MNV was performed if needed. We confirmed that there was no blood flow signal from the lower margin of the outer plexiform layer to above the RPE layer in the structural OCT + OCTA images to ensure that type 2 and 3 NV were not included. MNV en-face images were cropped using the open-source GNU Image Manipulation Program (GIMP) (version 2.8.14) to manually segment the MNV and eliminate surrounding signals.

Quantitative image analysis
All MNV slabs from OCTA en-face images were assigned unique numbers and testers (MC and SWK) were blinded to information about the study participants. To assess quantitative changes that occurred during the treatment process, AngioTool was used to analyse the MNV images as described in our previous study, with the following threshold parameters: 30 and 255, vessel thickness: 5, and removal of small particles: 80 [7]. AngioTool can identify vascular configurations based on user-defined parameters such as vessel diameter and intensity and does not involve a binarization process. AngioTool semi-automatically delineates and skeletonizes the vascular structure [16–18] and can obtain the following metrics: (1) vessel area; (2) total length of the vessel, defined as the sum of Euclidean distances between the pixels of all vessels; (3) total number of junctions, referring to the internal branching points of vessels; and (4) total number of endpoints, defined as the total number of open-ended segments (including the end of the mature vessel and the end of the sprouting new vessel) in a vessel. The junction density and endpoint density were calculated using the number of junctions and endpoints, respectively, divided by the total length of the vessel (n/mm) [19].

Statistical analyses
Data are shown as mean ± standard deviation (SD). The Statistical Package for the Social Sciences version 22 software program (IBM Corp., Armonk, NY, USA) and Prism 7 (GraphPad Software Inc., San Diego, CA, USA) was used for statistical and graphical analyses. Nonparametric analysis was selected after confirming that the quantitative metrics in this study did not follow a Gaussian distribution. Quantitative metrics of MNV at the baseline and T3 were compared between the two subgroups by a Mann-Whitney test and included in a binary logistic regression to identify risk factors related to early recurrence. A one-way repeated measures ANOVA (RM-ANOVA) with Greenhouse–Geisser correction and Tukey's multiple comparison test was used for the evaluation of changes in quantitative metrics according to the time course of treatment. P-values of less than 0.05 were considered to be statistically significant.

RESULTS
A total of 45 eyes of 45 patients (31 men and 14 women) were finally included in the study, with a mean age of 70.83 ± 9.97 (range: 50–88) years. The logMAR BCVA values were 0.456 ± 0.287 at baseline, 0.322 ± 0.279 at T3, and 0.317 ± 0.288 at one year after the third IVI (both $p < 0.001$ vs. baseline, RM–ANOVA). The mean time from T3 to R was 4.73 ± 3.61 months and the mean number of total IVIs performed from baseline to one year after the third IVI was 5.82 ± 1.39 injections (including the three loading injections).

Group comparison
Details of the comparison of patient demographics between the two groups are presented in eTable 1. Twenty-four and 21 patients were included in groups 1 and 2, respectively. There were no significant differences in terms of age, sex, or laterality. A comparison of the logMAR BCVA values between the two groups revealed no difference at baseline, T3, or one year after the third IVI. The mean time from T3 to R was 2.70 ± 0.69 months in group 1 and 6.97 ± 4.19 months in group 2. Quantitative OCTA metrics at baseline and T3 of the two groups are shown in Table 1. Patients in group 1 were characterized by a higher number of endpoints ($p = 0.015$) and greater endpoint density ($p = 0.035$) in MNV compared with group 2 at baseline. After the three loading

Table 1. Quantitative variables of NV associated with the early recurrence using binary logistic regression analysis.

	Group 1 (N = 24)	Group 2 (N = 21)	p value		
	mean (SD)	mean (SD)	Group comparison*	Univariate†	Multivariate‡
Baseline					
MNV area (mm²)	1.59 (1.07)	1.07 (0.57)	0.130	0.062	0.099
Total MNV length (mm)	30.45 (20.78)	18.95 (10.70)	0.115	0.058	0.115
Total junction number	110.86 (90.39)	67.56 (39.89)	0.267	0.086	0.149
Total endpoint number	115.90 (60.25)	60.25 (37.17)	0.015	0.020	0.012**
Junction density (n/mm)	3.46 (0.95)	3.57 (0.72)	0.649	0.714	NA
Endpoint density (n/mm)	4.13 (1.28)	3.25 (0.80)	0.035	0.031	0.044
T3					
MNV area (mm²)	1.36 (1.00)	0.74 (0.46)	0.014	0.021	0.351
Total MNV length (mm)	24.45 (19.18)	13.30 (8.84)	0.014	0.027	0.115
Total junction number	79.00 (43.89)	43.89 (31.71)	0.042	0.036	0.149
Total endpoint number	87.71 (77.66)	51.53 (41.62)	0.024	0.040	0.924
Junction density (n/mm)	3.22 (0.63)	3.24 (0.83)	0.732	0.929	NA
Endpoint density (n/mm)	3.61 (1.04)	3.88 (1.42)	0.826	0.474	NA

SD standard deviation, *MNV* macular neovascularization, *T3* 1 month after third intravitreal anti-VEGF injection.
*Mann–Whitney test.
†Binary logistic regression to identify risk factors related to early recurrence (group 1).
‡The variables that had an association in the univariate logistic regression analysis ($p < 0.2$) were included in the multivariate analysis using the forward conditional method to establish a proper multivariate model. Multivariate model summary; Hosmer and Lemeshow test; chi-squared test = 10.593, $p = 0.157$, −2 log likelihood = 35.474.
**Exp(B) = 1.023, 95% CI: 1.005–1.042; $p = 0.012$.

injections, group 1 showed larger area ($p = 0.014$) and longer length ($p = 0.014$) of MNV and a greater number of junctions ($p = 0.042$) and endpoints ($p = 0.024$), but both the density of junctions and endpoints did not vary between the two groups ($p = 0.732$ and $p = 0.826$). Figure 1 shows examples of time-course changes of eyes in each group and images analysed by AngioTool (version 0.6a; National Cancer Institute, Centre for Cancer Research, Bethesda, MD, USA).

Risk factors for early recurrence
Univariate binary logistic regression results are presented in Table 1. Total number of endpoints and endpoint density at baseline were significantly correlated with group 1 status ($p = 0.020$ and 0.031); MNV area, length, and total number of junction and endpoints points at T3 were also significantly correlated with group 1 status ($p = 0.021, 0.027, 0.036$ and 0.040). Meanwhile, multivariate analyses revealed that the total endpoint number [Exp(B) = 1.023, 95% confidence interval (CI): 1.005–1.042; $p = 0.012$] at baseline was only significantly related to group 1 status. The ROC curve for the total endpoint number at baseline to predict early recurrence is shown in eFigure 2. The area under the curve was 0.725 ($p = 0.017$, 95% CI: 0.561–0.888).

Change in qualitative MNV metrics in OCTA during IVI treatment
Mean MNV area measured on ICGA was 3.77 ± 3.35 mm at baseline and 3.12 ± 3.35 mm at T3. Mean MNV area measured on OCTA by AngioTool was 1.54 ± 0.92 mm at baseline and 1.28 ± 0.87 mm at T3. Pearson's correlation test showed a close relationship between the two measurements (correlation coefficient [CC] = 0.791 and $p < 0.001$ before treatment, CC = 0.617, $p < 0.001$ at T3).

The time-course changes of MNV metrics in OCTA are presented in Fig. 2 and eTable 2. Area, length, total junctions, and total endpoints of MNV were significantly decreased from baseline to T2. At T3, area and length results showed no difference from those at T2. In the recurrence stage (R), area, length, total endpoints and

junction of MNV were significantly increased compared to at T3 ($p = 0.004, 0.005, < 0.001, 0.03$) and showed no significant difference from baseline ($p = 0.67, 0.49, 0.68$ and 0.99).

Changes in MNV preceding exudation in each group
Quantitative changes of MNV in each group are presented in Fig. 3 and eTable 2. Unlike in the total study cohort, changes in the area and length in MNV at R were observed only in group 2. In group 1, the total endpoint number increased significantly at R (101.70 ± 56.52) as compared with at T3 (80.14 ± 56.70; $p = 0.005$). Meanwhile, the MNV area, length, and junction number at R were increased relative to at T3 but not to a statistically significant degree. In group 2, the number of total endpoints was significantly higher at P (68.00 ± 51.18) than at T3 (49.71 ± 38.49; $p = 0.01$), while there was no difference observed between at P and R (75.00 ± 56.37; $p = 0.695$). Meanwhile, the MNV area and length did not change at P (0.89 ± 0.57 mm² and 14.78 ± 11.25 mm) as compared with at T3 (0.78 ± 0.43 mm² and 12.91 ± 7.63 mm) but did exhibit significant increases at R (1.15 ± 0.58 mm² and 19.54 ± 11.77 mm; $p = 0.024$ and $p = 0.049$, respectively). The time-course changes in MNV seen in group 2 suggested that the endpoint number of MNV increased before exudation recurrence, followed by an increase in MNV size and length at exudation recurrence. Figure 4 shows examples of the time-course changes of eyes in group 2.

DISCUSSION
We investigated multiple quantitative metrics used in previous studies obtained from OCTA and focused on predictive features related to early recurrence after loading IVIs and preceding changes prior to exudation recurrence during the PRN protocol follow-up. Anti-VEGF prunes back the peripheral pericyte uncovered vessels in MNV lesions, leading to reductions in size, length, and the number of peripheral open-ended vessels (endpoints) [20]. Pilotto et al. reported that type 1 MNV showed significant reduction in area at 48 hours after IVI and larger MNV vessels
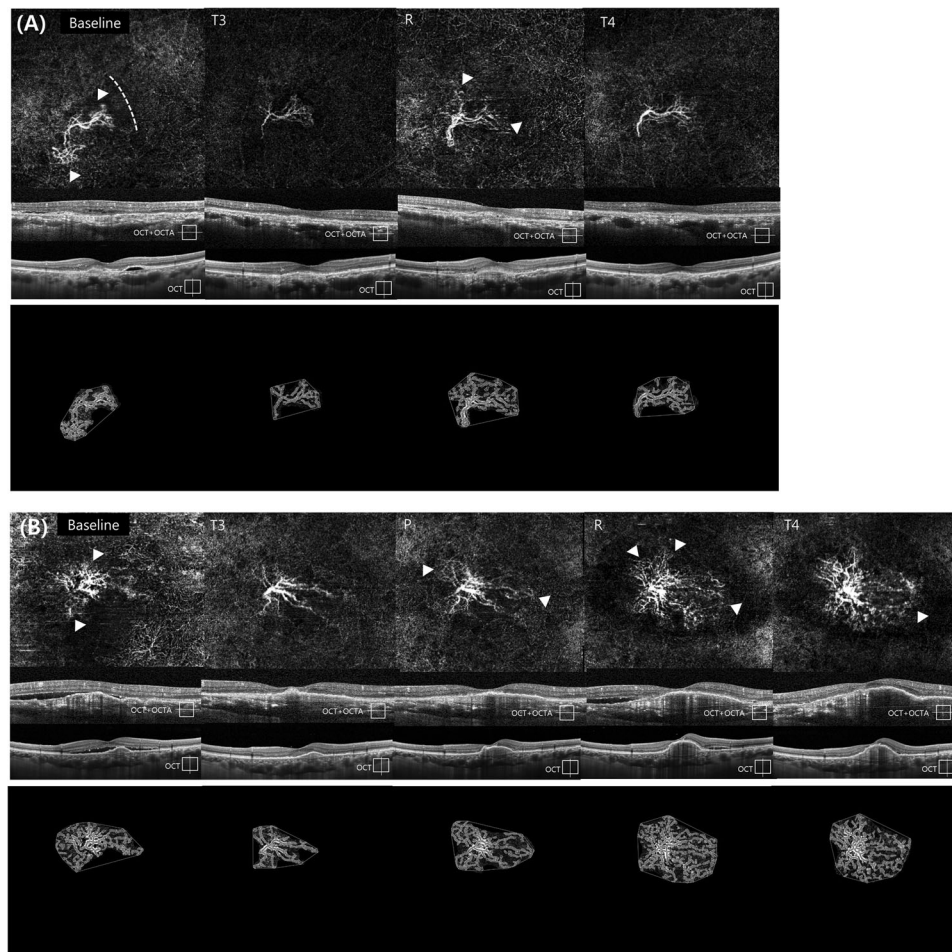
Fig. 1 Changes in MNV in OCTA during the treatment course. A, B Upper row: *En-face* OCTA image of the NV slab with OCT + OCTA images (horizontal image at fovea) and structural OCT images (vertical image at fovea). On OCT + OCTA images, yellow dots show flow signal and red dotted lines represent the segmentation line for the MNV slab (external limiting membrane and Bruch's membrane). Lower row: the images obtained from AngioTool analysis. A skeletonized vessel (red line), junction point (blue dot), vessel area (outer yellow along the vessels), and endpoint (point of the open-ended vessel) can be seen. **A** The changes in MNV in OCTA during the treatment course of a patient diagnosed with type 1 NVAMD who was included in group 1 (early recurrence). Tiny branching capillaries (white arrowhead) with perilesional halo (yellow dashed line) were found at baseline. (T3) After three loading injections, peripheral branching capillaries had significantly regressed and the size and length of MNV showed remarkable reductions. (R) Significant increases in peripheral sprouting vessels (white arrowhead) and the size of MNV at two months after T3 with focal subretinal fluid on structural OCT are visible. (T4) After the fourth IVI, peripheral tiny branching and the size of MNV showed partial regression as compared with at R. **B** A patient included in group 2. (T3) Tiny branching capillaries at baseline were dramatically regressed after three loading injections. The size and length of MNV showed remarkable reductions. (P) Peripheral sprouting vessels (white arrowhead) appeared at two months after T3, with slight enlargement of PED size but without exudative changes. (R) Significant increases in the size and length of MNV appeared with exudation recurrence. (T4) After the fourth IVI, peripheral tiny branches showed partial regression, but the size of MNV was not diminished relative to at R. The open-source GNU Image Manipulation Program (GIMP) (version 2.8.14, https://www.gimp.org/) was used.

showed less reduction than fine MNV vessels [12]. Studies on OCTA assessment of MNV after IVI reported that type 1 MNV showed a relatively small reduction in area as compared with those with type 2 after IVI and the MNV area reduction after IVI was significant in treatment-naïve patients but not in treated patients for one year with the PRN protocol [11, 21]. In our study, MNV features of patients with treatment-naïve continuously exhibited decreases in size, length, and numbers of endpoints and junction points during the first three loading IVIs, which increased again at exudation recurrence.

Previously, there have been a number of attempts to identify MNV characteristics related to exudative activity [8, 9, 22, 23] and many researchers have also tried to distinguish features of "active" and "quiescent" MNV [24–26]. In this study, we aimed to investigate the characteristics of treatment-naïve MNV in the active state, which showed early exudation recurrence after

loading IVIs. Logistic regression suggested that the greater the total number of endpoints at baseline, the earlier the recurrence of exudation after loading IVIs [Exp(B) = 1.023, 95% CI: 1.005–1.042; p = 0.012]. The endpoints include open-ended points of mature and new sprouting vessels and represent sprouting activity of NV peripheral lesions and lesion complexity. This could possibly be used as a predictive marker for early recurrence after IVI.

During consecutive analysis, the total endpoint number also showed the most notable growth at exudation recurrence among all metrics. Interestingly, during subgroup analysis, at about three months after the third loading injection ("R" in the early recurrence group and "P" in the late recurrence group, respectively), the total number of endpoints in OCTA increased in both the early and late recurrence groups, suggesting the occurrence of significant MNV alterations preceding exudation in the latter group. Meanwhile, a significant increase in the total length and
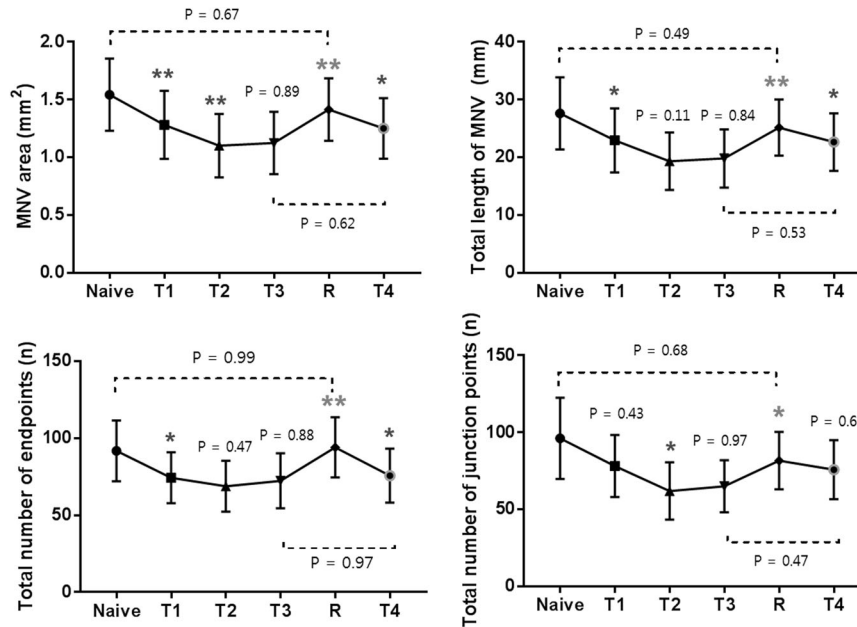
Fig. 2 Time-course changes of MNV metrics in OCTA. All values are presented in eTable 2. A repeated-measures ANOVA was used for the evaluation of changes according to the time course of treatment. A red asterisk is used to indicate a significant ($p < 0.05$) increase in the value as compared with the previous time point (**$p < 0.001$). A blue asterisk is used to indicate a significant ($p < 0.05$) decrease in the metrics relative to the previous value (**$p < 0.001$). Other time-point comparisons of metrics are presented as dotted lines.
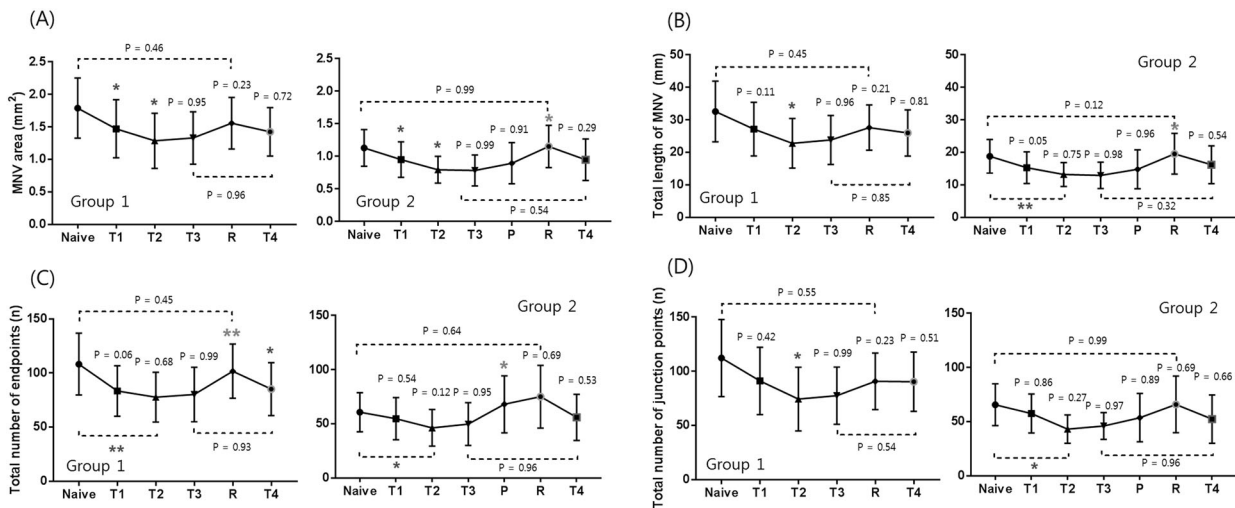

Fig. 3 The time-course changes of MNV metrics in OCTA in each group. Red and blue asterisks are used to indicate significance ($p < 0.05$) increases and decreases in values as compared with the previous time point (**$p < 0.001$). Other time-point comparisons of metrics are presented as dotted lines. (**A**) MNV area (mm²), (**B**) Total length of MNV (mm), (**C**) Total number of endpoints, (**D**) Total number of junction points.

area of MNV at exudation recurrence followed an increase in the total number of endpoints at two months before exudation recurrence (R).

In NVAMD eyes treated with an anti-VEGF therapeutic, rebound of unbound VEGF causes destabilization of the vessels and loosening of interendothelial cells through which endothelial cells emigrate and angiogenesis occur. The tip cells sprouting from the periphery of vessels are mainly stimulated by VEGF, with subsequent proliferation to the stalk cells [27]. These tiny peripheral sprouting vessels grow into immature capillaries that may be correlated with the exudative activity of MNV [20]. The stalk cells are then rearranged through migration and elongation, forming matured vessels covered with pericyte and smooth muscle cells [28]. The high degree of flow stress in the vascular

lumen promotes structural remodelling together with vessel wall expansion, which is known as arteriogenesis [29, 30]. The histological sequence of MNV growth might support the suggestion that an increase in peripheral open-ended vessels, representing sprouting activity, may be useful as a predictive biomarker for exudation recurrence.

Still, a consensus regarding ways of predicting exudation on OCT images by assessing NMV morphology in OCTA has not been achieved so far. Many researchers have indicated peripheral fine vessels, peripheral arcade, loops, and perilesional halo to be predictive factors, but Von der Emde et al. [17]. contended that patients with quiescent MNV who had never before been treated nor experienced exudation showed small-calibre vessels (100%) and peripheral arcade (100%); further, the median vessel length
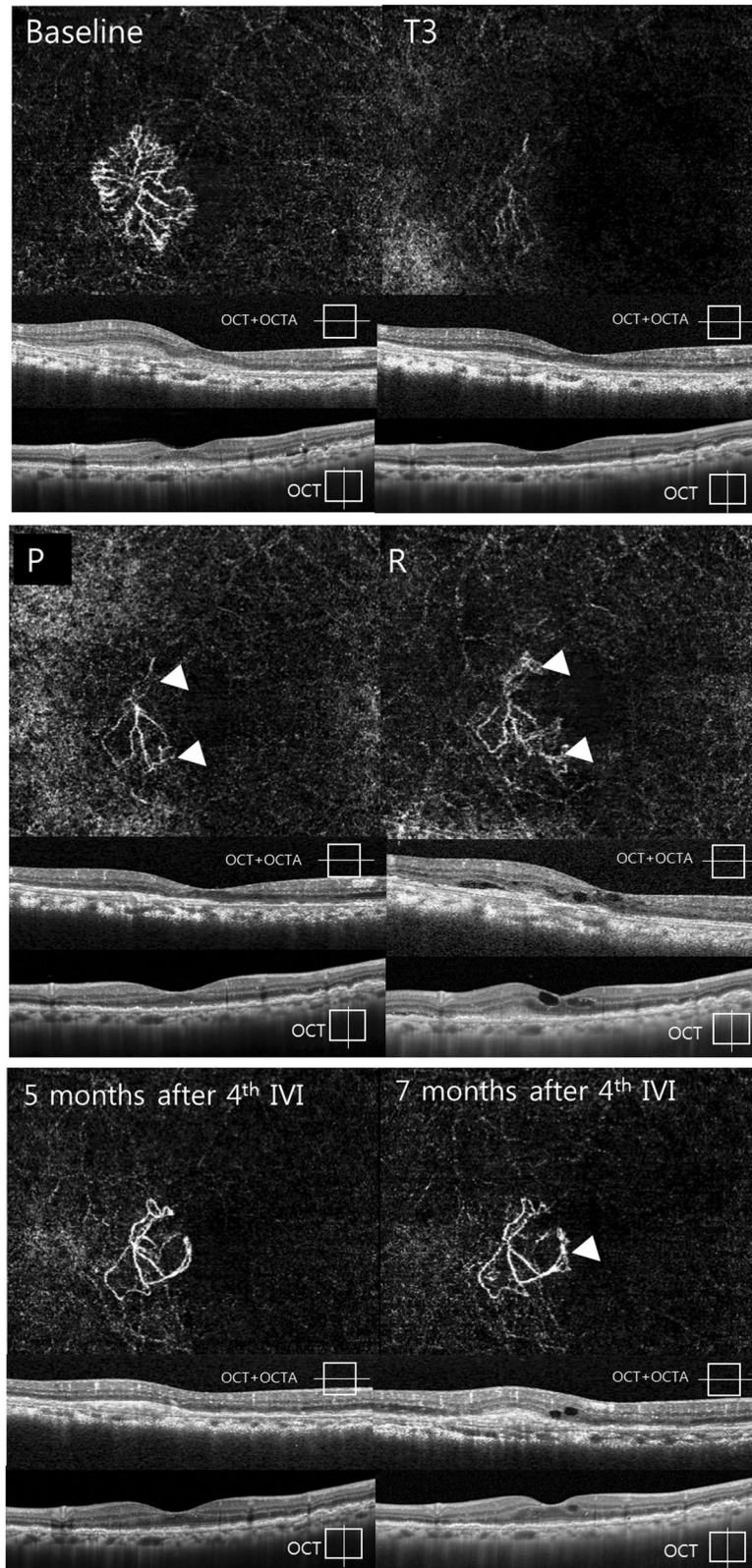
was much longer in patients with quiescent MNV (75.1 mm) than in those with active MNV (26.7 mm). In consecutive observations of MNV in the present study, we observed a definite increase in the MNV metrics of size, length, and number of endpoints at the point of exudation recurrence when compared with at T3. Given

these results, we think that our study enhances awareness regarding the use of OCTA during observations of serial changes in MNV, which is preferable over simply performing morphological assessments at a single time point to predict exudative changes. In particular, the increase in the number of endpoints that

Fig. 4 A case of the time-course changes in group 2. En-face OCTA with OCT + OCTA images (horizontal image at fovea) and structural OCT images (vertical image at fovea) during the treatment course of a patient diagnosed with type 1 NVAMD included in group 2 (late recurrence). On OCT + OCTA images, yellow dots show flow signal and red dotted lines represent the segmentation line for the MNV slab (external limiting membrane and Bruch's membrane). (Baseline) In the baseline state, the lacy wheel appearance of type 1 MNV was confirmed and, after three loading IVIs, (T3) the NV was much regressed to an indistinct appearance. (P) At the visit two months after T3, exudation was not observed on structural OCT, while the MNV size was slightly increased and peripheral vessel growth was suspected (white arrowhead) on OCTA. (R) After two months without additional IVIs, intraretinal fluid was recurred and the peripheral branching vessels were markedly increased. Enhancement of the NV area was also observed due to vessel growth at the periphery of vessels. (Bottom row, left) Changes in OCTA during long-term follow-up (not included in the quantitative analysis of this study) of this patient showed the shape of a filamentous vessel with loop but without exudation at five months after the fourth IVI. (Bottom row, right) After two months, the peripheral sprouting vessel was observed again and exudation had also recurred. The open-source GNU Image Manipulation Program (GIMP) (version 2.8.14, https://www.gimp.org/) was used.

◀

suggested precedence changes prior to exudation is considered to be a predictive biomarker of exudation recurrence and could be useful in treatment decision-making.

The PRN regimen with aflibercept showed somewhat poor visual acuity results as compared with monthly dosing in NVAMD [5]. Augsburger et al. reported that, in a retrospective analysis of 1,332 eyes, the ranibizumab and aflibercept T&E group experienced greater improvement in vision and more stable visual acuity during the maintenance period relative to those patients in the ranibizumab PRN treatment group [31]. Veritti et al., also reported inferior visual acuity in PRN arm than fixed regimen at month 8 and 12 during treatment using the aflibercept [32]. Although our study does not compare treatment protocols, patients with the PRN regimen showed a preceding change on OCTA before exudation, which suggests the need for proactive treatment.

There are several limitations to this study, such as its retrospective nature; small number of subjects; and selective bias given that treatment-naïve patients who had large PEDs and submacular haemorrhage, which made for poor segmentation in OCTA, were excluded (12/63; 19.0%) from analysis. Blood flow below the signal threshold on OCTA may not be detected, and MNV segmentation may not cover the whole MNV volume. For this reason, MNV area may differ on ICGA and OCTA; in this study, the MNV area measured by ICGA was larger than that measured by OCTA in this study. This difference in MNV area measurement has also been shown in previous studies, and the possibility of area overestimation on ICGA has been raised due to leakage of dye [33, 34]. The Angiotool used for OCTA imaging in this study calculates area by delineation of the outline of the MNV, versus ICGA, which measures the entire boundary of the MNV membrane. In addition, it was not possible to determine whether the changes in MNV were caused solely by the PRN protocol because no comparison between treatment protocols was conducted. However, by comparing two groups with different durations to recurrence, this study presents a novel perspective on consecutive changes during exudation recurrence after three loading injections.

In conclusion, we herein suggest that the number of open-ended vessels in the lesion periphery in MNV patients in the treatment-naïve state could be related to earlier recurrence of exudation. A consecutive analysis suggested the number of open-ended vessels in the lesion periphery to be an active marker of exudation and precedes changes that result in exudation recurrence. Serial MNV observations in the treatment-naïve state and during IVI treatment could be a useful method for treatment decision-making and surveillance.

SUMMARY

What was known before

- Macular neovascularization in age-related macular degeneration with exudation was reported to decrease in terms of the area, segment length, and fractal dimensions after anti-vascular endothelial growth factor treatment and to increase on these same metrics when exudation recurred.
- The morphological feature of macular neovascularization which related with exudation were reported such as tiny vessel, tangled appearance, peripheral arcade.

What this study adds

- *Consecutive analysis This study analyzed neovascularization in consecutive optical coherence tomography angiography images during three loading anti-VEGF injections and exudation recurrence of neovascular Age-related macular degeneration.
- *Quantitative values of macular neovascularization Authors found that the number of open-ended vessels in the lesion periphery is a predictive marker for earlier recurrence and an active marker of exudation and preceding changes before exudation recurrence in AMD.

REFERENCES

1. Cheung LK, Eaton A. Age-related macular degeneration. Pharmacotherapy. 2013;33:838–55.
2. Heier JS, Brown DM, Chong V, Korobelnik JF, Kaiser PK, Nguyen QD, et al. Intravitreal aflibercept (VEGF trap-eye) in wet age-related macular degeneration. Ophthalmology. 2012;119:2537–48.
3. Rosenfeld PJ, Heier JS, Hantsbarger G, Shams N. Tolerability and efficacy of multiple escalating doses of ranibizumab (Lucentis) for neovascular age-related macular degeneration. Ophthalmology. 2006;113:623.e621.
4. Kertes PJ, Galic IJ, Greve M, Williams G, Baker J, Lahaie M, et al. Efficacy of a treat-and-extend regimen with ranibizumab in patients with neovascular age-related macular disease: a randomized clinical trial. JAMA Ophthalmol. 2020;138:244–50.
5. Richard G, Monés J, Wolf S, Korobelnik JF, Guymer R, Goldstein M, et al. Scheduled versus pro re nata dosing in the VIEW trials. Ophthalmology. 2015;122:2497–503.
6. Holz FG, Figueroa MS, Bandello F, Yang Y, Ohji M, Dai H, et al. RAnibizumab treatment in treatment-naive neovascular age-related macular degeneration: results from luminous, a global real-world study. Retina. 2020;40:1673–85.
7. Choi M, Kim SW, Yun C, Oh J. OCT angiography features of neovascularization as predictive factors for frequent recurrence in age-related macular degeneration. Am J Ophthalmol. 2020;213:109–19.
8. Hikichi T, Agarie M, Kubo N, Yamauchi M. Predictors of recurrent exudation in choroidal neovascularization in age-related macular degeneration during a treatment-free period. Retina. 2020;40:2158–65.
9. Solecki L, Loganadane P, Gauthier AS, Simonin M, Puyraveau M, Delbosc B, et al. Predictive factors for exudation of quiescent choroidal neovessels detected by OCT angiography in the fellow eyes of eyes treated for a neovascular age-related macular degeneration. Eye (Lond) 2020.
10. Faatz H, Farecki ML, Rothaus K, Gutfleisch M, Pauleikhoff D, Lommatzsch A. Changes in the OCT angiographic appearance of type 1 and type 2 CNV in exudative AMD during anti-VEGF treatment. BMJ Open Ophthalmol. 2019;4: e000369.
11. Miere A, Oubraham H, Amoroso F, Butori P, Astroz P, Semoun O, et al. Optical coherence tomography angiography to distinguish changes of choroidal

neovascularization after Anti-VEGF therapy: monthly loading dose versus pro re nata regimen. J Ophthalmol. 2018;2018:3751702.

12. Pilotto E, Frizziero L, Daniele AR, Convento E, Longhin E, Guidolin F, et al. Early OCT angiography changes of type 1 CNV in exudative AMD treated with anti-VEGF. Br J Ophthalmol. 2019;103:67–71.

13. Giovanni Staurenghi FB, Andrea Giani. Clinical Applications of Diagnostic Indocyanine Green Angiography. Ryan's Retina 6th edn. (Elsevier Inc., 2018). pp. 46-47.

14. Holmen IC, Konda SM, Pak JW, McDaniel KW, Blodi B, Stepien KE, et al. Prevalence and severity of artifacts in optical coherence tomographic angiograms. JAMA Ophthalmol. 2020;138:119–26.

15. Coscas GJ, Lupidi M, Coscas F, Cagini C, Souied EH. Optical coherence tomography angiography versus traditional multimodal imaging in assessing the activity of exudative age-related macular degeneration: a new diagnostic challenge. Retina. 2015;35:2219–28.

16. Roberts PK, Nesper PL, Gill MK, Fawzi AA. Semiautomated quantitative approach to characterize treatment response in neovascular age-related macular degeneration: a real-world study. Retina. 2017;37:1492–8.

17. von der Emde L, Thiele S, Pfau M, Nadal J, Meyer J, Möller PT, et al. Assessment of exudative activity of choroidal neovascularization in age-related macular degeneration by OCT angiography. Ophthalmologica. 2020;243:120–8.

18. Zudaire E, Gambardella L, Kurcz C, Vermeren S. A computational tool for quantitative analysis of vascular networks. PLoS One. 2011;6:e27385.

19. Takeuchi J, Kataoka K, Ito Y, Takayama K, Yasuma T, Kaneko H, et al. Optical coherence tomography angiography to quantify choroidal neovascularization in response to aflibercept. Ophthalmologica. 2018;240:90–8.

20. Spaide RF. Optical coherence tomography angiography signs of vascular abnormalization with antiangiogenic therapy for choroidal neovascularization. Am J Ophthalmol. 2015;160:6–16.

21. Kim JM, Cho HJ, Kim Y, Jung SH, Lee DW, Kim JW. Responses of types 1 and 2 neovascularization in age-related macular degeneration to anti-vascular endothelial growth factor treatment: optical coherence tomography angiography analysis. Semin Ophthalmol. 2019;34:168–76.

22. Coscas F, Lupidi M, Boulet JF, Sellam A, Cabral D, Serra R, et al. Optical coherence tomography angiography in exudative age-related macular degeneration: a predictive model for treatment decisions. Br J Ophthalmol. 2019;103:1342–6.

23. Bae K, Kim HJ, Shin YK, Kang SW. Predictors of neovascular activity during neovascular age-related macular degeneration treatment based on optical coherence tomography angiography. Sci Rep. 2019;9:19240.

24. Al-Sheikh M, Iafe NA, Phasukkijwatana N, Sadda SR, Sarraf D. Biomarkers of neovascular activity in age-related macular degeneration using optical coherence tomography angiography. Retina. 2018;38:220–30.

25. Nesper PL, Soetikno BT, Treister AD, Fawzi AA. Volume-rendered projection-resolved OCT angiography: 3D lesion complexity is associated with therapy response in wet age-related macular degeneration. Invest Ophthalmol Vis Sci. 2018;59:1944–52.

26. Uchida A, Hu M, Babiuch A, Srivastava SK, Singh RP, Kaiser PK, et al. Optical coherence tomography angiography characteristics of choroidal neovascularization requiring varied dosing frequencies in treat-and-extend management: An analysis of the AVATAR study. PLoS One. 2019;14:e0218889.

27. Carmeliet P. Mechanisms of angiogenesis and arteriogenesis. Nat Med. 2000;6:389–95.

28. Potente M, Gerhardt H, Carmeliet P. Basic and therapeutic aspects of angiogenesis. Cell. 2011;146:873–87.

29. Tzima E, Irani-Tehrani M, Kiosses WB, Dejana E, Schultz DA, Engelhardt B, et al. A mechanosensory complex that mediates the endothelial cell response to fluid shear stress. Nature. 2005;437:426–31.

30. Deindl E, Quax PHA. Arteriogenesis and Therapeutic Angiogenesis in Its Multiple Aspects. Cells 2020;9.

31. Augsburger M, Sarra GM, Imesch P. Treat and extend versus pro re nata regimens of ranibizumab and aflibercept in neovascular age-related macular degeneration: a comparative study. Graefes Arch Clin Exp Ophthalmol. 2019;257:1889–95.

32. Veritti D, Sarao V, Missiroli F, Ricci F, Lanzetta P. Twelve-month outcomes of intravitreal aflibercept for neovascular age-related macular degeneration: fixed versus as-needed dosing. Retina. 2019;39:2077–83.

33. Costanzo E, Miere A, Querques G, Capuano V, Jung C, Souied EH. Type 1 choroidal neovascularization lesion size: indocyanine green angiography versus optical coherence tomography angiography. Invest Ophthalmol Vis Sci. 2016; 57: 307–13.

34. Cicinelli MV, Cavalleri M, Consorte AC, Rabiolo A, Sacconi R, Bandello F, et al. Swept-source and spectral domain optical coherence tomography angiography versus dye angiography in the measurement of type 1 neovascularization. Retina. 2020;40:499–506.

AUTHOR CONTRIBUTIONS

MC and SWK were involved in the conception and design of the study. MC and SWK were involved in data collection and literature research. SWK, CY, JHO and JO were involved in the interpretation and critical revision of the article. MC was involved in the data analysis and drafting of the manuscript. MC, SWK, CY, JHO and JO were involved in the final approval of the article.

FUNDING

COMPETING INTERESTS

The authors declare no competing interests.

ADDITIONAL INFORMATION

Supplementary information The online version contains supplementary material available at https://doi.org/10.1038/s41433-021-01879-2.

Correspondence and requests for materials should be addressed to Seong-Woo Kim.

Reprints and permission information is available at http://www.nature.com/reprints

Publisher's note Springer Nature remains neutral with regard to jurisdictional claims in published maps and institutional affiliations.